



4-1-13

FAILURE OF THE COHESIVE SILTY SOIL SUBJECTED TO CYCLIC SHEAR

Sukeo O-HARA¹ and Tetsuro YAMAMOTO²

¹Ube Technical College, Yamaguchi, Japan

²Department of Civil Engineering, Technical Junior College, Yamaguchi University, Yamaguchi, Japan

SUMMARY

The cyclic simple shear tests, using a shaking table are performed on two kinds of saturated silty loams with different cohesion. Also, the tests of saturated Toyoura sand are carried out to compare with the test results of saturated silty loams. From the tests, it becomes clear that the failure of the silty loams induced by cyclic shear is essentially similar to liquefaction of sand. Also, a method of determining such as failure of the silty loams is presented. Second, based on the test results, the failure of a saturated silty loam deposit induced by cyclic shear is investigated analytically.

INTRODUCTION

O-hara and Matsuda¹⁾ have shown experimentally that a saturated cohesive soil subjected to cyclic shear failed similar to liquefaction of sand. But, due to the presence of cohesion, the pore water pressure developed in the cohesive soil reached effective confining pressure only temporarily. Thus, it may be considered that the increase of pore water pressure developed in cohesive soil by cyclic shear depends on cohesion, and its failure is complex compared with that of sand. Therefore, the method of determining such as failure of cohesive soil has not been established as yet.

So, in this paper, in order to establish a method of determining the failure of cohesive soil by cyclic shear, a series of cyclic simple shear tests, using the shaking table are performed on the saturated silty loams with different cohesion. Furthermore, the failure of a silty loam deposit induced by cyclic shear is investigated analytically, using these test results.

CYCLIC SIMPLE SHEAR TEST ON FAILURE OF SILTY LOAM

Test Device The test apparatus used in this study is shown in Fig.1. This is the dynamic simple shear test apparatus having Kjellman's type shear box fixed on the shaking table. This is the same type as that used in previous experiment²⁾. In the tests, to prepare the saturated silty loam specimen by consolidation, the doughnut lead weight (10) is used. A vertical stress acting on a surface of the specimen is 49kPa. The specimen is 30cm in diameter and about 4cm in height. To prevent the lateral expansion of specimen and to induce the simple shear deformation, four polyvinyl chloride rings are stacked around the specimen covered with a rubber membrane of 1mm thickness. A size of the ring is 1cm in thickness, and in-

ner and outer diameters are 30.2cm, 35.0cm, respectively. The shear strain double amplitude of specimen during shaking is controlled to a maximum in about 17% by the stopper (1).

Samples and Test Method Samples used in this test are two kinds of silty loams and Toyoura sand. Physical properties and strength parameters are shown in Table 1. Silty loams (I) and (II) were prepared by drying and sieving the soils obtained from in situ. Though silty loam(I) closely resembles silty loam(II) in the grain distribution, cohesion of silty loam(I) is 1.6 times that of silty loam(II).

In order to obtain the saturated silty loam specimen, after filling the de-aired slurry sample into the shear box, it was consolidated for 20 hours under a vertical stress of 49kPa. The saturated sand specimen was obtained by pouring little by little wet sand into a water filled rubber membrane. Table 2 shows void ratio, e , water content, w , and degree of saturation, S_r for each specimen. Thereafter, the cyclic simple shear tests were carried out by applying the specimen horizontal sinusoidal vibration with a frequency of 3Hz and constant amplitude. During the testing the acceleration of the shaking table, the pore water pressure, and the shear displacement amplitude of the specimen were measured by each transducer shown in Fig.1 and these measurements were recorded on a pen-written oscilloscope.

Determination of Failure of Silty Loam Figs.2(a) and 2(b) show typical test records of silty loam(I) and Toyoura sand, respectively. In both the records σ'_{v0} and $(\sigma'_{v0})_m$ are initial vertical stresses acted on a bottom of the specimen without and with considering rocking of the specimen during shaking, respectively. τ is shear stress amplitude. As seen in Fig.2(b), Toyoura sand specimen liquefied at a required number of cycles of vibration. The shear strain double amplitude γ_D at the occurrence of liquefaction reaches about 17%. Here the occurrence of liquefaction is defined by the condition in which the pore water pressure developed in the specimen is equal to σ'_{v0} . On the other hand, in silty loam(I) shown in Fig.2(a) though the pore water pressure gradually increases with increasing shear strain, liquefaction does not occur even if when γ_D reaches about 17%. This same behavior was also recognized in silty loam(II). Thus, it is considered that the failure of the silty loams occurred by the increase of pore water pressure during cyclic shear, and this fact is similar to liquefaction of sand.

Next, the strain at such as failure of the silty loam was determined by the following method. First, after obtaining the vertical stress σ'_v and the shear stress amplitude τ acting on the bottom of the specimen at $\gamma_D=8\%$, 10%, 15%, and 17% from records of Fig.2(a) etc., their values were plotted on a σ'_v versus τ graph. As an example, the result of $\gamma_D=15\%$ for silty loam(I) is shown in Fig.3. In this figure symbol \bigcirc represents the experimental value and the straight line was obtained using a least squares method. This line is regard as a dynamic rupture line in the case considering that the specimen failed at $\gamma_D=15\%$. From this rupture line, the dynamic angle of internal friction ϕ_D is found to be 19.3° and the dynamic cohesion C_D to be 2.9kPa. ϕ_D and C_D of silty loam(I) thus obtained are plotted versus γ_D in Fig.4. It is found in this figure that the dynamic cohesion becomes maximum when γ_D is 15%. Namely, it can be considered that the cohesion fully mobilized at $\gamma_D=15\%$. After all, the dynamic strength parameter; i.e., ϕ_D and C_D of silty loam(I) obtained from Fig.4 are 19.3° and 2.9kPa, respectively. Also, it was found that the dynamic cohesion of silty loam(II) becomes maximum at $\gamma_D=15\%$, and ϕ_D and C_D at $\gamma_D=15\%$ are 17.3° and 2.0kPa, respectively. Therefore, we concluded that the failure of the silty loam subjected to cyclic shear occurs at $\gamma_D=15\%$.

Dynamic Strength and Pore Water Pressure Buildup at Failure Fig.5 shows the relationship between the number of cycles for γ_D up to 15%(i.e., failure) n_{15} and the stress ratio $\tau/(\sigma'_{v0})_m$ for each sample. From this figure, due to cohesion stress ratio for the silty loams are 2-3 times larger than that of the sand. Fig.

6 shows the relationship at the failure between the pore water pressure ratio, $(u/\sigma'_{v0})_{15}$ and $\tau/(\sigma'_{v0})_m$. It is seen in Fig.6 that $(u/\sigma'_{v0})_{15}$ developed in the sand becomes 1.0 for all the stress ratios, but $(u/\sigma'_{v0})_{15}$ of both the silty loams decreases with increasing the stress ratio, and does not never become 1.0. That is, when the stress ratios are about 0.1 and 0.3, the pore water pressure ratios at the failure of the silty loams become to about 0.8 and 0.4, respectively.

From the above mentioned test results, it is said that the failure of the silty loam induced by cyclic shear is related to the decrease of effective stress due to the increase of pore water pressure and the magnitude of shear stress. Consequently, it can be concluded that when the stress ratio acting on the silty loam becomes smaller, its failure occurred by cyclic shear is essentially similar to liquefaction of sand.

ANALYSIS OF FAILURE OF A SILTY LOAM DEPOSIT INDUCED BY CYCLIC SHEAR

Method of Calculation A saturated silty loam deposit with 20m in thickness and the physical properties of the silty loam, used in this analysis are shown in Fig. 7. The properties of this silty loam were assumed to be the same as those of silty loam(I). The El Centro earthquake record(1940), the simulated seismic wave, and the sinusoidal acceleration having constant amplitude and a period of 0.33sec are used as the base motion. The simulated seismic wave with a maximum acceleration $1.0m/s^2$ is shown in Fig.8.

The calculation of pore water pressure developed in the silty loam deposit by cyclic shear is the same as that described in detail in our previous paper³⁾. Therefore, we shall mention it only briefly in this paper. The distribution of shear stress developed in the deposit during every half periods of the seismic wave was calculated from Eq.(1), using Newmark's β -method. The equation(1) was deduced by modeling the deposit to the lumped mass system.

$$[M] \cdot \ddot{u}(t) + [C] \cdot \dot{u}(t) + [K] \cdot u(t) = -[M] \cdot \ddot{u}_g(t) \quad (1)$$

in which $[M]$ =mass matrix, $[C]$ =damping matrix, $[K]$ =stiffness matrix, u =displacement vector, \ddot{u}_g =acceleration vector, t =time.

The pore water pressure developed in the deposit under undrained conditions was obtained by adding the amount of pore water pressure, u_m every half cycles obtained by substituting the value of maximum shear stress in Eq.(2). This equation was derived by the relationship of the amount of increase of pore water pressure and stress ratio for silty loam(I) obtained from the cyclic simple shear tests.

$$u_m/\sigma'_{v0} = (-0.009 + 0.066 \cdot \tau/\sigma'_{v0}) \cdot n \quad (\tau/\sigma'_{v0} > 0.15) \quad (2)$$

Equivalent Number of Uniform Cycles Required to Cause Failure By considering the test results mentioned above, it was assumed that the silty loam deposit subjected to cyclic shear also failed when the pore water pressure ratio reached in the range of 0.4-0.8. As shown in Fig.9, because the amount of pore water pressure developed in the deposit is the largest at depth(z)=5m, first the relationship between the maximum acceleration amplitude of seismic wave, a_{max} and the maximum pore water pressure ratio, $(u/\sigma'_{v0})_{max}$ at $z=5m$ was examined. Both the relationships at $z=3m$ and $15m$ are also shown in Fig.9. It can be read from the curves in Fig.9 that a_{max} of the simulated seismic wave in case of that $(u/\sigma'_{v0})_{max}$ at $z=5m$ reached 0.4 and 0.8 are $1.7m/s^2$ and $2.6m/s^2$, respectively. Also, in the El Centro wave, a_{max} in case of that $(u/\sigma'_{v0})_{max}$ at $z=5m$ reached 0.4 and 0.8 are found to be $1.9m/s^2$ and $3.0m/s^2$, respectively.

Next, in order to obtain equivalent number of uniform cycles required to cause the failure of the deposit, the same calculation was made on the case of the

sinusoidal acceleration with amplitude of $a(=\beta \cdot a_{\max})$ as the base motion. β represents the ratio of acceleration amplitude of the sinusoidal wave(a) to the maximum acceleration amplitude of the seismic wave(a_{\max}) in case that the deposit failed. Fig.10 shows the relationship between β and equivalent number of uniform cycles n_e which $(u/\sigma'_{v0})_{\max}$ becomes 0.4 and 0.8. It is seen in Fig.10 that when β is the same, n_e for the sinusoidal wave equivalent to the simulated seismic wave is a little larger than n_e for that equivalent to the El Centro wave. Furthermore, the relationship between β and n_e is not much affected by the limited value of $(u/\sigma'_{v0})_{\max}$ required to cause the failure of the deposit.

Fig.11 shows the relationship between the stress ratio τ/σ'_{v0} which the deposit failed and n_e obtained by the calculation. The measured values for silty loam(I) shown in Fig.11 were obtained from the relationship between the stress ratios at $(u/\sigma'_{v0})_{\max}=0.4$ and 0.8 obtained from Fig.6, and n_e which was given as the values of n_{15} corresponding to the stress ratios obtained from Fig.5. It seems from Fig.11 that the data points plotted lie almost in the calculated curves. So, we proposed that equivalent number of uniform cycles n_e can be given by Fig.10. As a result, n_e for the desired β values are summarized in Table 3. In Table 3, for example, in the case of $\beta=0.65$ for the simulated seismic wave n_e is found to be 11.5 cycles for $(u/\sigma'_{v0})_{\max}=0.4$ and to be 13 cycles for $(u/\sigma'_{v0})_{\max}=0.8$.

CONCLUSIONS

The failure of two kinds of saturated silty loams with different cohesion induced by cyclic shear was investigated by a series of cyclic simple shear tests, using the shaking table. Furthermore, from these test results, equivalent number of uniform cycles required to cause the failure of a silty loam deposit by cyclic shear was calculated. Main conclusions obtained are summarized as follows.

- (1) The failure of silty loams induced by cyclic shear is due to the increase of pore water pressure, and is essentially similar to liquefaction of sand. The increase of pore water pressure is inverse to the amplitude of shear stress. Also, the pore water pressure ratio developed in the silty loams at the failure ranged from 0.4 to 0.8.
- (2) Because the dynamic cohesion of silty loams becomes maximum when the shear strain double amplitude is 15%, the strain at failure was determined as 15%.
- (3) Due to cohesion the stress ratios required to cause the failure of silty loams are about 2-3 times that of the sand.
- (4) When the acceleration amplitude of the sinusoidal wave is 0.65 times the maximum acceleration amplitude of the simulated seismic wave in case in which the deposit failed, equivalent number of uniform cycles are 11.5 and 13 cycles when the limited pore water pressure ratios are 0.4 and 0.8, respectively.

ACKNOWLEDGMENTS

The writers would like to express their gratitude to Messrs. Y. Okada, K. Sumita and Y. Imaoka, the former students at Yamaguchi University, for their helps during the experiments.

REFERENCES

- 1) O-hara, S. and Matsuda, H.(1978), "Dynamic Shear Strength of Saturated Clay", Proc. of the Japan Society of Civil Engineers, Vol.274, pp.69-78(in Japanese).
- 2) O-hara, S., Kotsubo, S. and Yamamoto, T.(1985), "Pore Pressure Developed in Saturated Sand Subjected to Cyclic Shear Stress under Partial-Drainage Conditions", Soils and Foundations, Vol.25, No.2, pp.45-56.
- 3) O-hara, S. and Yamamoto, T.(1986), "Fundamental Study of Gravel Pile Method for Preventing Liquefaction", Proc. of the 8th European Conference on Earthquake Engineering, Vol.2, pp.41-48.

Table 1 Physical properties and strength parameters of samples.

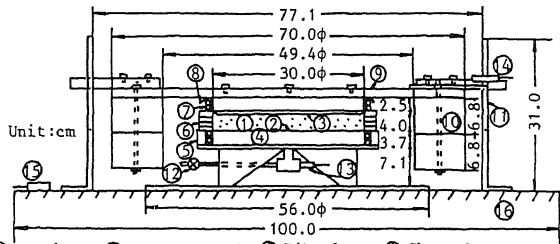
	Silty loam(I)	Silty loam(II)	Toyoura sand
G_s	2.586	2.939	2.633
D_{max} (mm)	0.84	0.84	0.84
D_{50} (mm)	0.027	0.025	0.260
U_c	11.7	10.0	1.6
e_{max}	-	-	1.005
e_{min}	-	-	0.631
WL(%)	55.9	NP	-
Wp(%)	32.1	27.8	-
I_p	23.8	-	-
ϕ (°)	$\phi_{cu}=22.1$	$\phi_{cu}=25.1$	$\phi_d=39.7$
C(kPa)	$C_{cu}=15.7$ ($e=1.262$)	$C_{cu}=9.8$ ($e=0.870$)	$C_d=0$ ($e=0.970$)

Table 2 e, w, and S_r of each specimen.

	Silty loam(I)	Silty loam(II)	Toyoura sand
e	1.419±0.047	0.852±0.038	0.819±0.014
w(%)	54.3±1.9	28.4±1.6	31.0±0.8
S_r (%)	97.4±2.6	97.3±1.7	99.3±0.7

Table 3 Equivalent number of uniform cycles n_e .

$(u/\sigma'_{vo})_{max}/\beta$	n_e			
	El Centro wave		Simulated seismic wave	
	0.8	0.4	0.8	0.4
0.80	8.5	7.5	10.0	9.0
0.65	10.5	10.5	13.0	11.5
0.60	11.5	11.5	14.0	12.5
0.50	14.0	14.5	17.0	16.5
0.40	19.5	20.5	24.5	24.0



- ① Specimen ② Porous metal ③ Rib plate ④ Shear box
- ⑤ Supporting plate ⑥ Polyvinyl chloride ring ⑦ O-ring
- ⑧ Rubber membrane ⑨ Loading plate ⑩ Lead weight ⑪ Stopper
- ⑫ Drainage valve ⑬ Pore water pressure transducer
- ⑭ Displacement transducer ⑮ Accelerometer ⑯ Shaking table

Fig.1 Test apparatus.

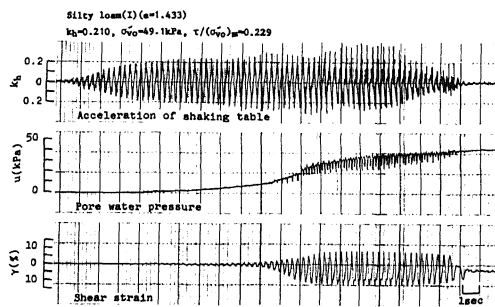


Fig.2(a) Typical test record of silty loam(I).

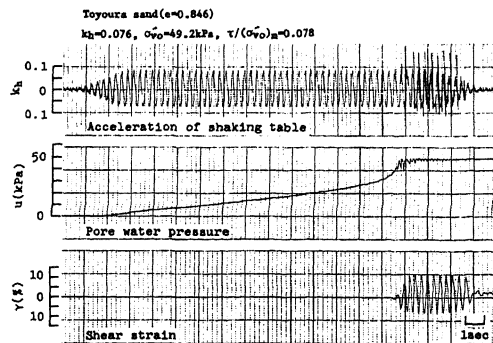


Fig.2(b) Typical test record of Toyoura sand.

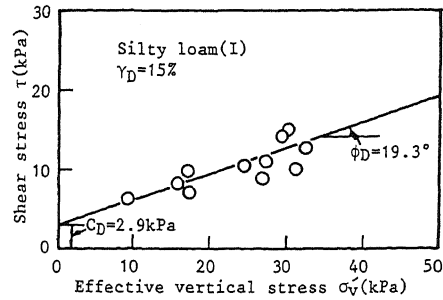


Fig.3 Relationship between σ'_v and τ .

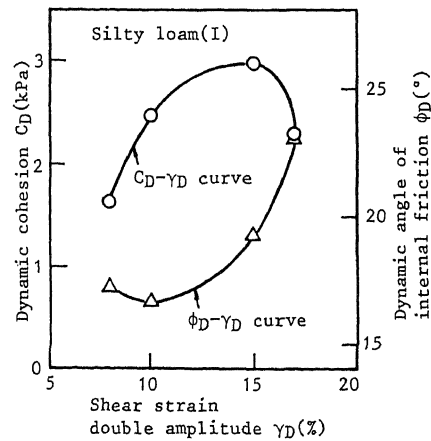


Fig.4 Relationship between C_D and ϕ_D , and γ_D (silty loam(I)).

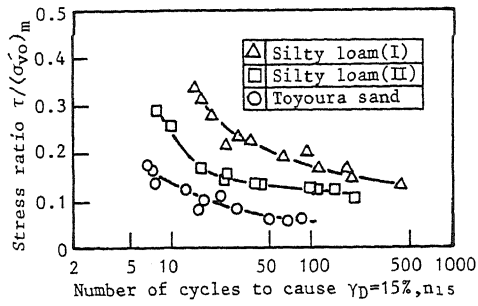


Fig.5 Relationship between $\tau/(\sigma'_{v0})_m$ and n_{15} .

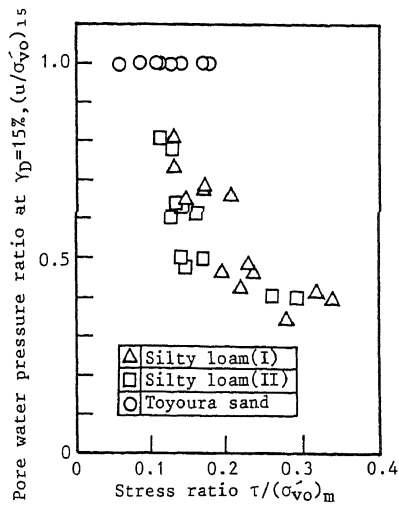


Fig.6 Relationship between $(u/\sigma'_{v0})_{15}$ and $\tau/(\sigma'_{v0})_m$.

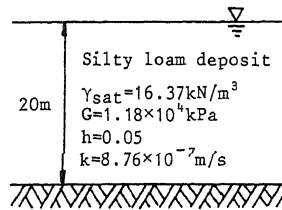


Fig.7 Silty loam deposit used in this analysis.

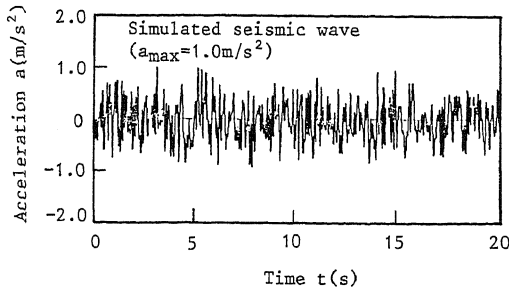


Fig.8 Simulated seismic wave with $a_{max}=1.0m/s^2$.

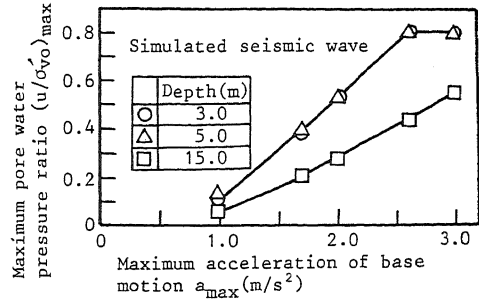


Fig.9 Relationship between $(u/\sigma'_{v0})_{max}$ and a_{max} .

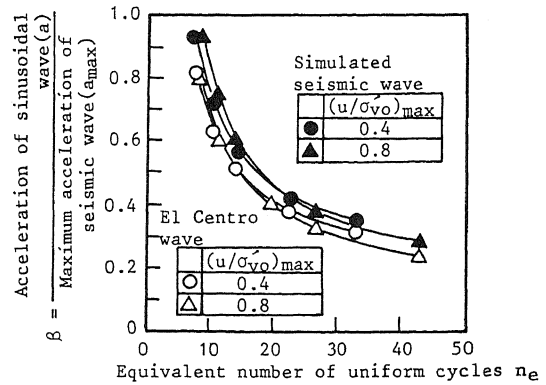


Fig.10 Relationship between β and n_e .

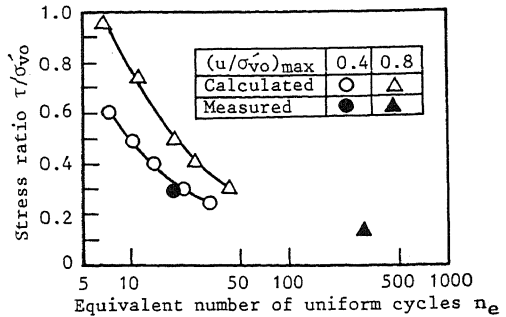


Fig.11 Relationship between τ/σ'_{v0} and n_e .